Preprints of the 19th World Congress
The International Federation of Automatic Control
Cape Town, South Africa. August 24-29, 2014

Nonlinear observer and controller design for sensorless operation of a continuously rotating energy harvester ⋆

K. Nunna[*], **T. T. Toh**[*], **P. D. Mitcheson**[*], **A. Astolfi**[*,†]

[*] *Department of Electrical and Electronic Engineering, Imperial College London, London SW7 2AZ*
[†] *The Dipartimento di Ingegneria Civile e Ingegneria Informatica, Università di Roma "Tor Vergata", Via del Politecnico, 1 00133 Rome, Italy*

Abstract: This paper presents the design of a nonlinear observer and a nonlinear feedback controller for sensorless operation of a continuously rotating energy harvester. A mathematical model of the harvester with its power electronic interface is discussed. This model is used to design an observer that estimates the mechanical quantities from the measured electrical quantities. The gains of the observer depend on the solution of a modified Riccati equation. The estimated mechanical quantities are used in a control law that sustains power generation across a range of source rotation speeds. The proposed scheme is assessed through simulations and experiments.

Keywords: Nonlinear observer, sensorless, energy harvester, nonlinear controller, Riccatti equation

1. INTRODUCTION

Energy harvesting devices have become a viable method of powering sensor networks and low-power electronics using ambient energy sources such as heat, solar, radio or vibration. Harvesters offer several advantages over conventional battery power sources like extended lifetime of operation, and clean energy generation (Paradiso and Starner, 2005). They have a wide range of applications from wearable biomedical sensors for health monitoring to condition monitoring of machinery. These applications makes energy harvesting an attractive research area given the growth of worlds population and its ever increasing demand for energy (Barker et al., 2013).

Eliminating sensors and transducers in the harvesters, thus enabling sensorless operation, reduces operational cost while increasing the ruggedness and reliability. Sensorless operation is used for on-line tool fault detection and in reporting faults in modern manufacturing industry (Franco-Gasca et al., 2006). Measuring mechanical quantities or operating states in energy harvesters still remains a challenging task due to the unavailability of access points. The existing approaches to sensorless operation are based on saliency, Kalman filter and model reference techniques (Rashed and Stronach, 2004). These techniques are computationally intensive, require special construction for estimation or require proper initialisation (Degner and Lorenz, 1998). This paper presents, as an example application, sensorless operation of a continuously rotating harvester, *i.e.* a rotational energy harvester.

⋆ This work is partially supported by the EPSRC Programme Grant Control For Energy and Sustainability EP/G066477.

The harvester is based on balancing the torque generated by the gravitational force and the motor torque acting on a suspended mass, see Toh et al. (2008). The sensorless control scheme discussed in Nunna et al. (2013) improves the efficiency of the harvester given in Toh et al. (2008) by estimating the mechanical quantities from the measured electrical quantities and using these in a nonlinear control law. The optimization problem *i.e.* generating maximum energy for a given source rotation speed is transformed into a stabilization problem; maintaining the angle of the suspended mass at an angle of $\pi/2$ rad to the vertical axis allows maximal power extraction.

This paper generalises the observer design in Nunna et al. (2013) by eliminating the requirement of any prior knowledge on the source rotation speed and extends it to the case in which the source rotation speed varies as a function of time. The observer gains depend on the solution of a modified algebraic Riccati equation. This makes it an attractive alternative to the design discussed in Nunna et al. (2013). The control design presented here is a variation of the one in Nunna et al. (2013) and maintains the angular position of the suspended mass at an angle of $\pi/2$ rad to the vertical axis for any source rotation.

The rest of the paper is organized as follows. Section 2 discusses the mathematical model of the harvester and its validation. The basics of the observer design technique are given in Section 3 together with their application to the harvester and the description of the control design procedure. Section 4 gives simulation results and Section 5 provides experimental evidence. The paper is concluded in Section 6 with suggestions for future work and some comments.

2. DEVELOPMENT AND VALIDATION OF THE HARVESTER'S MATHEMATICAL MODEL

In this section, for completeness, we recall the mathematical model for the rotational energy harvester, and describe its validations steps which have been presented in Nunna et al. (2013)

The rotational energy harvester consists of a DC generator with its stator coupled to a continuously rotating source and a semicircular mass m attached to the rotor at a distance l from the axis of rotation (see Figure 1). When power is drawn from the generator the torque between the stator and rotor (motor torque) is counteracted by the torque generated by the gravitational force acting on the offset mass (gravitational torque). The difference between these two torques creates a difference in the angular speeds of the stator and the rotor that can be tapped off as power. The excess generated power is stored in an energy reservoir in the form of a supercapacitor, see Toh et al. (2008). To ensure optimal power transfer from the harvester to the load, the load resistance, R_L, should be closely matched to the harvester's armature resistance, R_a. Since the input impedance of a boost converter R_{in} can be controlled by varying its duty cycle, δ (see (Toh et al., 2008))

$$R_{in} = R_L(1-\delta)^2\,, \tag{1}$$

it is used as a power electronic interface circuit between the harvester and the load.

The experimental set-up for the harvester and the interface electronics is illustrated in Figure 2. In this set-up the source rotation is connected to a gear box with a conversion ratio of 1 : 4.4 to generate a higher voltage at low source rotation speeds. The values for the various mechanical constants and the circuit components used in the experimental model are given in Table 1. For a more detailed explanation of the construction and the choice of the circuit components, see Toh et al. (2008) and references therein.

Table 1. Component values for the experimental set-up.

k_E	8.6436 rad/sV
k_T	0.0610 mNm/A
g	9.8 m/s^2
m	100 g
l	0.03 m
L	680 μH
C	4.53 mF
r_m	0.04 m
R_a	11.2 Ω
Microprocessor	PIC18F1320
Maxon motor	118733

From the free body diagram of the offset mass in Figure 1, the torque balance on the mass attached to the rotor of the harvester is given by

$$J\dot{\omega} = \Gamma_M - mgl\sin\theta\,, \tag{2}$$

where J is the moment of inertia of the semicircular mass calculated as $\frac{2mr_m^2}{5}$, ω is the angular velocity, and θ is the deflection angle of the mass measured from the vertical axis. The motor torque Γ_M is calculated as

$$\Gamma_M = -k_T I_{in}\,,$$

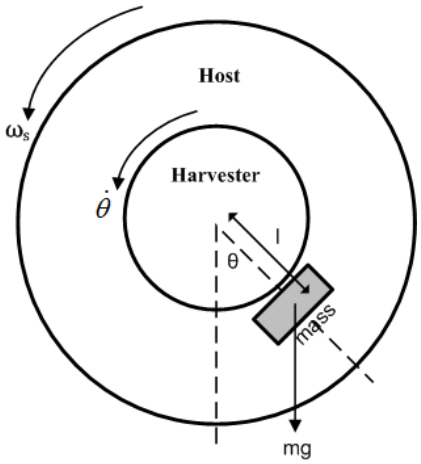

Fig. 1. A schematic diagram of the rotational energy harvester.

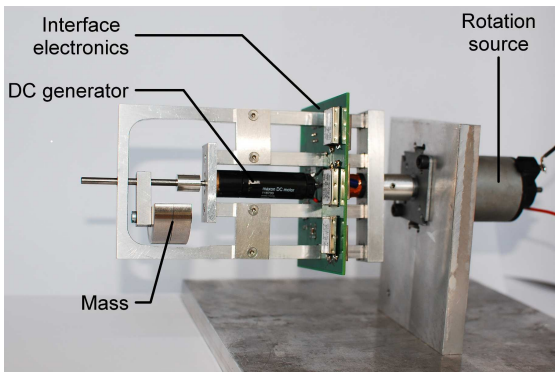

Fig. 2. Experimental set-up of the rotational energy harvester.

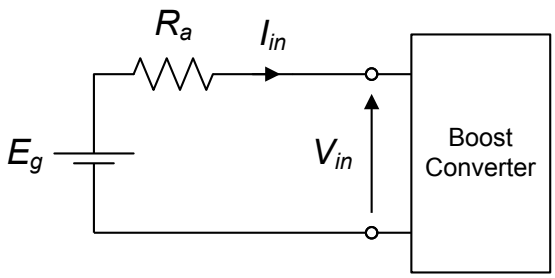

Fig. 3. Equivalent circuit diagram to calculate I_{in}.

where k_T is the torque constant of the motor, and I_{in} is the current drawn by the DC generator. The negative sign indicates that the current flows out of the generator and into the boost converter. The voltage generated by the harvester, E_g, when it is attached to a continuously rotating source at a speed ω_s is calculated as

$$k_E(\omega_s - \omega)\,, \tag{3}$$

where k_E is the "motor constant" of the DC generator.

Application of Kirchoff's voltage law to the circuit diagram in Figure 3 and use of the relations $I_{in} = \frac{V_{in}}{R_{in}}$ and (1) yield

$$V_{in} = \frac{k_E(\omega_s-\omega)(1-\delta)^2 R_L}{(R_a + (1-\delta)^2 R_L)}\,. \tag{4}$$

The standard averaged model that describes the dynamics of the boost converter composed of an inductor and a supercapacitor is, (see Rodriguez et al. (2000) and references therein)

$$\dot{I}_L = -\frac{(1-\delta)V_C}{L} + \frac{1}{L}\underbrace{\frac{k_E(\omega_s-\omega)(1-\delta)^2R_L}{(R_a+(1-\delta)^2R_L)}}_{V_{in}}, \quad (5)$$

$$\dot{V}_C = \frac{I_L}{C} - \frac{V_C}{R_L C}, \quad (6)$$

where V_C is the voltage across the supercapacitor of capacitance C, I_L is the current flowing through the inductor of inductance L, and V_{in} is as in (4).

Using equations (4)-(6), the mathematical model of the harvester with the interface circuit is given by

$$\begin{bmatrix}\dot{x}_1\\ \dot{x}_2\\ \dot{x}_3\\ \dot{x}_4\end{bmatrix} = \begin{bmatrix} x_2 \\ -\frac{mgl\sin x_1}{J} + \frac{k_E k_T(\omega_s - x_2)}{J(R_a+(1-\delta)^2R_L)} \\ -\frac{(1-\delta)x_4}{L} + \frac{k_E(\omega_s-x_2)(1-\delta)^2R_L}{L(R_a+(1-\delta)^2R_L)} \\ \frac{(1-\delta)x_3}{C} - \frac{x_4}{R_L C}\end{bmatrix} \quad (7)$$

where x_1, x_2 describe the angular position θ and the angular velocity ω of the mass, respectively, and x_3, x_4 describe the inductor current I_L and the output capacitor voltage V_C of the boost converter, respectively.

It can be inferred from the $\dot{x}_2$ equation that the operating condition: $x_1 = \pm\pi/2$ and $x_2 = 0$ maximises the amount of gravitational torque, *i.e.* $\frac{mgl\sin x_1}{J}$, generated by the mass and ensures the largest difference in rotational speeds between the stator and rotor, *i.e.* $\omega_s - x_2$. As the source rotation increases, maintaining the angular position of the mass at $\pi/2$ prevents it from flipping over and synchronising with the source rotation.

The validation of the model is carried out by calculating the relative errors between the estimated current/voltage and measured current/voltage when the experimental set-up and the simulated model are driven by the same input. These errors have been reported to be below 0.2% in Nunna et al. (2013), suggesting that the mathematical model (7) with the parameters of Table 1 gives an accurate description of the system.

3. NONLINEAR OBSERVER AND CONTROLLER DESIGN

The observer design is based on the method described in Astolfi et al. (2008); Karagiannis and Astolfi (2005). We aim to estimate accurately the mechanical parameters *i.e.* angular position, angular velocity and source rotation speed from the measured electrical variables *i.e.* inductor current and capacitor voltage. We first revisit the main result for observer design of Astolfi et al. (2008); Karagiannis and Astolfi (2005) and then discuss its application to the rotational energy harvester.

3.1 General reduced-order observer design

Consider a nonlinear, time-varying, system described by equations of the form

$$\dot{\eta} = f_1(\eta, y, t), \quad (8)$$

$$\dot{y} = f_2(\eta, y, t), \quad (9)$$

where $\eta(t) \in \mathbb{R}^n$ is the unmeasured part of the state and $y(t) \in \mathbb{R}^m$ is the measurable output. It is assumed that the system's trajectories starting at time t_0 are defined for all times $t \geq t_0$.

Definition 1. The dynamical system

$$\dot{\hat{\eta}} = \alpha(y, \hat{\eta}, t), \quad (10)$$

with $\eta(t) \in \mathbb{R}^p$, $p \geq n$, is called an observer for the system (8)-(9) if there exists mappings

$$\beta(\cdot) : \mathbb{R}^n \times \mathbb{R}^m \times \mathbb{R}^p \to \mathbb{R}^p \text{ and } \phi(\cdot) : \mathbb{R}^n \to \mathbb{R}^p,$$

with $\phi(\cdot)$ left-invertible, such that the manifold

$$\mathcal{M}_t = (\eta, y, \hat{\eta}) \in \mathbb{R}^n \times \mathbb{R}^m \times \mathbb{R}^p : \beta(y, \hat{\eta}, t) = \phi(\eta)$$

is positively invariant *i.e.* all trajectories of the extended system (8)-(9)-(10) that start on the manifold $\mathcal{M}_t$ remain there for all future times $\tau \geq t$, and is attractive *i.e.* all trajectories of the extended system that start in a neighbourhood of $\mathcal{M}_t$ asymptotically converge to $\mathcal{M}_t$.

To construct an observer of the form given in Definition 1 we require the solution of a PDE in β. In particular β should be such that the signal $z = \beta(\hat{\eta}, y, t) - \phi(\eta, y, t)$ converges asymptotically to zero, uniformly in η, y, t.

3.2 Third order observer design

This section describes the observer design based on the method outlined in Section 3.1 and a modification of an algebraic Riccati equation. The observer estimates the angular position of the mass, the angular velocity of the mass and the input source rotation speed that is assumed constant, from the duty cycle, the measured current and the measured voltage.

To streamline the statement of the proposition let

$$A = \begin{bmatrix} 0 & 1 & 0 \\ -mgl & -v^2 & v^2 \\ 0 & 0 & 0 \end{bmatrix}, \quad C = [1\ 0\ 0],$$

$$K = [0\ \rho\ -\rho], \qquad P = \begin{bmatrix} 0 & \frac{mgl}{J} & 0 \end{bmatrix}^\top.$$

Proposition 1. Consider the system

$$\begin{aligned}
\dot{\hat{x}}_1 &= \hat{x}_2 + \beta_2(x_3) - \frac{\partial\beta_1(x_3)}{x_3}x_{3o}, \\
\dot{\hat{x}}_2 &= -\frac{mgl\sin(\hat{x}_1 + \beta_1(x_3))}{J} - \frac{\partial\beta_2(x_3)}{x_3}x_{3o} \\
&\quad - \left(\frac{k_E k_T(\hat{\omega}_s + \beta_3(x_3) - \hat{x}_2 - \beta_2(x_3))}{R_a + (1-\delta)^2 R_L}\right), \\
\dot{\hat{\omega}}_s &= -\frac{\partial\beta_3(x_3)}{x_3}x_{3o}, \quad (11)
\end{aligned}$$

with states $[\hat{x}_1(t),\ \hat{x}_2(t),\ \hat{\omega}_s]^\top \in \mathbb{R}^3$, inputs $x_3(t) \in \mathbb{R}$, $x_4(t) \in \mathbb{R}$, $\delta(t) \in [0,\ 1]$, with

$$x_{3o} = -\frac{(1-\delta)x_4}{L} + \rho(\hat{\omega}_s + \beta_3(x_3) - \hat{x}_2 - \beta_2 x_3)\,,$$
$$\beta_i(x_3) = b_i x_3 \text{ for } i = 1\,,2\,,3\,, \tag{12}$$

where $\rho = \dfrac{k_E(1-\delta)^2 R_L}{L(R_a + (1-\delta)^2 R_L)}$. Let $B = [b_1\ b_2\ b_3]^\top$. Suppose there exists a positive definite matrix $X \in \mathbb{R}^{3\times 3}$ such that

$$A^\top X + XA + \frac{XPP^\top X}{(J+1)^2} + C^\top C - 2K^\top K < 0\,. \tag{13}$$

Then the selection $[b_1\ b_2\ b_3]^\top = -X^{-1}K^\top$ is such that $\lim_{t\to\infty}(\hat{x}_1(t) + \beta_1(x_3) - x_1(t)) = 0$, $\lim_{t\to\infty}(\hat{x}_2(t) + \beta_2(x_3) - x_2(t)) = 0$ and $\lim_{t\to\infty}(\hat{\omega}_s(t) + \beta_3(x_3) - \omega_s(t)) = 0$ *i.e.* the system (11) is an asymptotically converging observer for the harvester (7).

Proof. Let $z = [\beta_1(x_3) + \hat{x}_1\,, \beta_2(x_3) + \hat{x}_2\,, \beta_3(x_3) + \hat{\omega}_s]^\top - [x_1\,, x_2\,, \omega_s]^\top$. The time derivative of z can be written in the form of a feedback interconnected system, namely

$$\begin{bmatrix}\dot{z}_1\\ \dot{z}_2\\ \dot{z}_3\end{bmatrix} = \left(\underbrace{\begin{bmatrix}0 & 1 & 0\\ -mgl & -v^2 & v^2\\ 0 & 0 & 0\end{bmatrix}}_{A} + \underbrace{\begin{bmatrix}b_1\\ b_2\\ b_3\end{bmatrix}}_{B}\underbrace{[0\ \rho\ -\rho]}_{K}\right)\begin{bmatrix}z_1\\ z_2\\ z_3\end{bmatrix} - \underbrace{\begin{bmatrix}0\\ \dfrac{mgL}{J}\\ 0\end{bmatrix}}_{P} u\,,$$
$$\zeta = z_1\,, \tag{14}$$

where $u = \Gamma(x_1, z_1)\zeta$, with $\Gamma = \underbrace{\dfrac{\sin(x_1+z_1) - \sin(x_1)}{z_1}}_{\Gamma_1} - J$ and $v^2 = \dfrac{k_E k_T}{J(R_a + (1-\delta)^2 R_L)}$. The system $u = \Gamma(x_1, z_1)\zeta$ has a L_2 gain $\|\Gamma\|_2$ which can be calculated by noting that the maximum of $|\Gamma|$ is such that

$$\frac{d\Gamma_1}{dz_1} = \frac{\cos(x_1+z_1)}{z_1} - \frac{\sin(x_1+z_1) - \sin(x_1)}{{z_1}^2} = 0\,,$$

which yields $\|\Gamma\|_2 \leq 1 + J$. Note now that the Riccati equation (13) with $B^\top X = -K$ can be rewritten as

$$A^\top X + XA + \frac{XPP^\top X}{(1+J)^2} + C^\top C - K^\top K - XBB^\top X + XBB^\top X + [K + B^\top X]^\top [K + B^\top X] < 0\,,$$

or equivalently as

$$(A+BK)^\top X + X(A+BK) + \frac{XPP^\top X}{(J+1)^2} + C^\top C < 0\,. \tag{15}$$

Therefore, if there exists a $X = X^\top > 0$ solving (15) then the L_2 gain of system (14) with input u and output ζ is less than $1 + J$. The asymptotic convergence claim then follows by invoking the small gain theorem (see Khalil (2002); Van der Schaft (1992); Willems (1971)).

Remark 1. The observer design presented can be extended to the case in which ω_s varies as a function of time. For instance, if $\omega_s = \omega_{s_0} + \omega_{s_1} t$, a 4^{th} order observer that estimates the "states" $x_1\,, x_2\,, \omega_{s_0}\,, \omega_{s_1}$ can be derived. Letting z be $[\beta_1(x_3)+\hat{x}_1\,, \beta_2(x_3)+\hat{x}_2\,, \beta_3(x_3)+\hat{\omega}_{s_0}\,, \beta_4(x_4)+\hat{\omega}_{s_1}]^\top - [x_1\,, x_2\,, \omega_{s_0}\,, \omega_{s_1}]^\top$ results in the matrices

$$A = \begin{bmatrix}0 & 1 & 0 & 0\\ -mgl & -v^2 & v^2 & 0\\ 0 & 0 & 0 & 1\\ 0 & 0 & 0 & 0\end{bmatrix}\,, \quad C = [1\ 0\ 0\ 0]\,,$$
$$K = [0\ \rho\ -\rho\ 0]\,, \qquad P = \begin{bmatrix}0 & \dfrac{mgl}{J} & 0 & 0\end{bmatrix}^\top\,.$$

Similarly to what is shown in Proposition 1, if there exists a positive definite matrix $X \in \mathbb{R}^{4\times 4}$ such that the modified ARE (13) has a solution, then the selection $[b_1\ b_2\ b_3\ b_4]^\top = -X^{-1}K^\top$ yields in an asymptotically converging observer.

3.3 Controller design

As discussed in Section 2, to optimise the performance of the harvester the angular position of the mass should be maintained at $\pi/2$ rad for a range of source rotation speeds. This enables continuous harvesting of energy from the source as the mass is prevented from flipping over and synchronising with the source rotation. The equations of the model in (7) suggest that the angular position of the mass x_1 can be adjusted by changing the amount of torque acting on it. This can be changed using the control variable δ. The proposed control law aims to hold the mass at $\pi/2$ rad using the observer design in Proposition 1 to estimate the mechanical quantities.

Proposition 2. Consider the rotational energy harvester system (7). The control law

$$\delta = 1 - \sqrt{\frac{k_E k_T}{\mu R_L} - \frac{R_a}{R_L}}\,,$$

where

$$\mu = -\frac{mgl(1-\sin x_1)}{\min(\varepsilon, \omega_s - x_2)} + \eta\,(\omega_s - x_2)\cos x_1 + \frac{mgl}{\omega_s}\,,$$

for $0 < \eta << 1$ and $0 < \varepsilon < 1$ globally asymptotically stabilizes the equilibrium $(\pi/2, 0)$ of the (x_1, x_2) subsystem. In addition $\delta(t) \in [0,\ 1]$ and $x_2(t) < \omega_s$ for all $t \geq 0$

Proof. The proof follows the lines used in Nunna et al. (2013).

Remark 2. The physical characteristics of the harvester along with the choice of δ as the control variable restrict the operational range of the harvester. This limitation can be overcome if a saturation control scheme such as $\delta = \min\left(\max\left(\mu, \dfrac{k_E k_T}{(R_L + R_a)}\right), \dfrac{k_E k_T}{R_a}\right)$ is used, see Nunna et al. (2013)

4. SIMULATION RESULTS

The observer in Proposition 1 has been implemented in Matlab with $b_1 = 0.004$, $b_2 = -0.04$ and $b_3 = 3.5$. The errors between the estimated angular position, angular

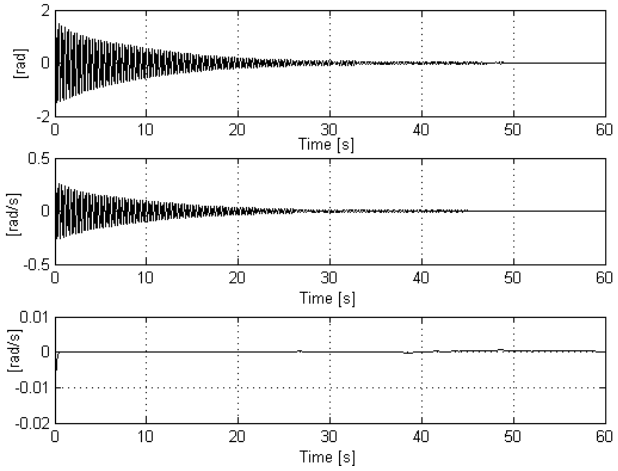

Fig. 4. Time histories of the estimation errors on the angular position of the mass (top), angular velocity of the mass (middle) and source rotation (bottom).

velocity, source rotation estimated from the filtered experimental data collected and the simulation data when they are subjected to the same inputs $\omega_s = 44\,\text{rad/s}$ and $\delta = 0.70$ are plotted in Figure 4. We compare the observer output from the experimental data and the simulated data due to the absence of sensors for measuring the angular position and the angular velocity in the experimental set-up. The sensors have not been incorporated in the set-up due to space and cost constraints. Figure 4 shows that the errors asymptotically converge to zero indicating the effectiveness of this observer design.

Figure 5(a) demonstrates the performance of the observer and controller scheme discussed in Proposition 1 and Proposition 2. This has been implemented in Matlab with $\omega_s = 44\,\text{rad/s}$ from $0 - 120\,\text{s}$ and $\omega_s = 51\,\text{rad/s}$ from $120 - 150\,\text{s}$. The output voltage obtained in simulations is higher than the voltage obtained from the experiment when it is subjected to the same variation in ω_s for a constant duty cycle $\delta = 0.70$ without the controller. This suggests that the proposed scheme improves the efficiency of the harvester. The controller varies the control input, δ to maintain the angular position of the mass at $\pi/2\,\text{rad}$ and the angular velocity of the mass at $0\,\text{rad/s}$ as required with a varying ω_s, see Figure 5(b).

5. EXPERIMENTAL IMPLEMENTATION OF THE OBSERVER-CONTROLLER DESIGN

To implement the observer on the experimental model the method in Proposition 1 is used. The source rotation speed is assumed to be a known constant due to the limited computational power available on the chip. Therefore we estimate only the angular position and velocity from the measured inductor current, the measured capacitor voltage and a fixed source rotation speed, see Nunna et al. (2013).

Using the observer design method discussed in Section 3, the dynamical system

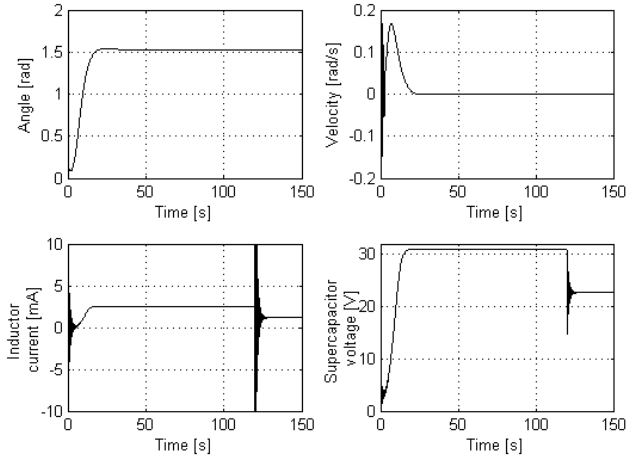

(a) Time histories of the angular position of the mass (top left), the angular velocity of the mass (top right), the inductor current (bottom left) and the supercapacitor voltage (bottom right).

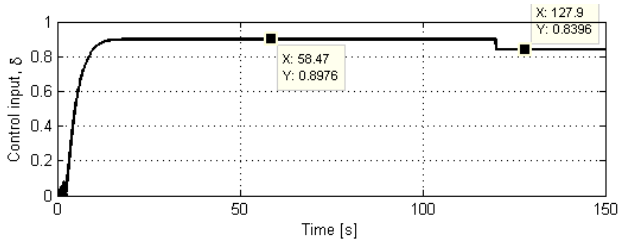

(b) Control input, δ.

Fig. 5. Performance of the third order observer and the nonlinear controller.

$$\dot{\hat{x}}_1 = \hat{x}_2 + \beta_2(x_3) - \frac{\partial \beta_1}{x_3} x_{3o}\,, \tag{16}$$

$$\dot{\hat{x}}_2 = -\frac{mgl\sin(\hat{x}_1 + \beta_1(x_3))}{J} - \frac{\partial \beta_2(x_3)}{x_3} x_{3o} - \left(\frac{k_E k_T(\omega_s - \hat{x}_2 - \beta_2)}{R_a + (1-\delta)^2 R_L}\right), \tag{17}$$

with states $[\hat{x}_1(t),\ \hat{x}_2(t)]^\top \in \mathbb{R}^2$, $b_1 > 0$, $b_2 < 0$, inputs: $x_3(t) \in \mathbb{R}$, $x_4(t) \in \mathbb{R}$, $\delta(t) \in [0,\ 1]$ and $\omega_s(t) \in \mathbb{R}$,

$$\beta_1(x_3) = \frac{b_1 - 1}{\rho} x_3\,,$$

$$\beta_2(x_3) = \left(\frac{b_2}{\rho} - \frac{k_E k_T}{\rho(R_a + (1-\delta)^2 R_L)} x_3\right),$$

$$x_{3o} = -\frac{(1-\delta)x_4}{L} + \rho(\omega_s - \hat{x}_2 - \beta_2)\,,$$

with $b_1 > 0$, $b_2 < 0$, is an asymptotically converging observer for the rotational energy harvester system (7).

5.1 Results

Figure 6 demonstrates the performance of the observer given by the equations (16) and (17) with filtered experimental data for $\omega_s = 90\text{rad/s}$, $\delta = 0.92$, $b_1 = 3$, and $b_2 = -7$. The estimated values from the observer are used to implement a variation of the control law in Proposition 2. Figure 7 illustrates the closed-loop performance of the

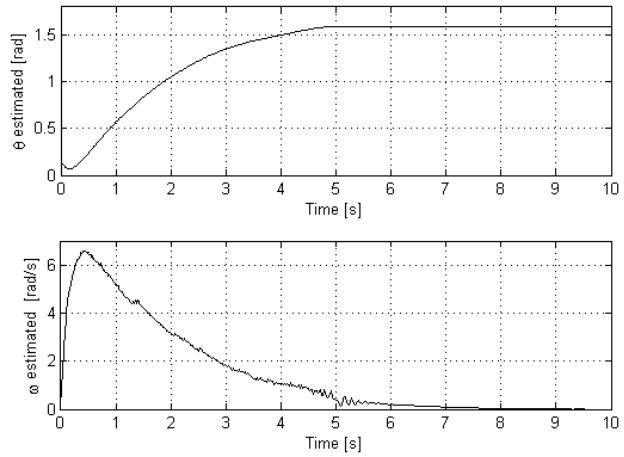

Fig. 6. Time histories of the angular position (top) and angular velocity (bottom) estimated from the filtered data collected from the experimental set-up.

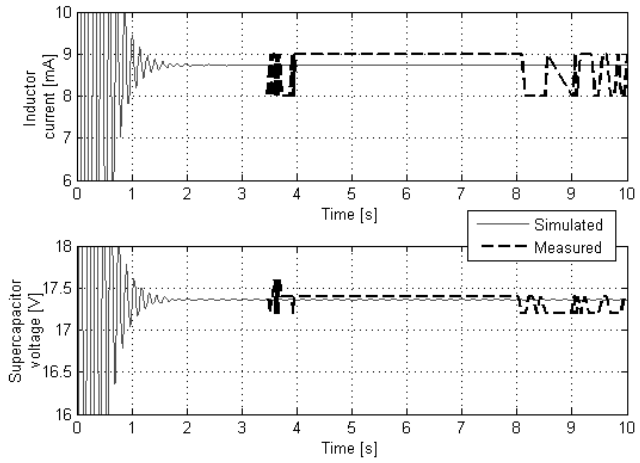

Fig. 7. Time histories of the angular position (top) and angular velocity (bottom) estimated from the filtered data collected from the experimental set-up.

proposed scheme in experiments and simulations. The data collected from the experiments are only available after 3s due to the self-powered nature of the harvester. This means that the transmission of data starts only after the harvester starts generating energy and storing it in the supercapacitors.

6. CONCLUSIONS

A model of a rotational energy harvester with its power electronic interface has been discussed. This model has been used for the design of an observer and a controller, the performances of which have been demonstrated via simulations and experiments. The proposed observer method can be adapted for other types of harvesters.

REFERENCES

Astolfi, A., Karagiannis, D., and Ortega, R. (2008). *Nonlinear and adaptive control with applications*. Springer.

Barker, T., Ekins, P., and Johnstone, N. (2013). *Global warming and energy demand*. Routledge.

Degner, M.W. and Lorenz, R.D. (1998). Using multiple saliencies for the estimation of flux, position, and velocity in ac machines. *IEEE Trans. Ind. Appl.*, 34(5), 1097–1104.

Franco-Gasca, L.A., Herrera-Ruiz, G., Peniche-Vera, R., de Jess Romero-Troncoso, R., and Leal-Tafolla, W. (2006). Sensorless tool failure monitoring system for drilling machines. *International Journal of Machine Tools and Manufacture*, 46(34), 381 – 386.

Karagiannis, D. and Astolfi, A. (2005). Nonlinear observer design using invariant manifolds and applications. In *Decision and Control, 2005 and 2005 European Control Conference.*, 7775–7780.

Khalil, H.K. (2002). *Nonlinear systems*, volume 3. Prentice hall Upper Saddle River.

Nunna, K., Toh, T.T., Mitcheson, P.D., and Astolfi, A. (2013). Sensorless estimation and nonlinear control of a rotational energy harvester. In *Journal of Physics: Conference Series*, volume 476, 012052. IOP Publishing.

Paradiso, J.A. and Starner, T. (2005). Energy scavenging for mobile and wireless electronics. *Pervasive Computing, IEEE*, 4(1), 18–27.

Rashed, M. and Stronach, A.F. (2004). A stable back-emf mras-based sensorless low-speed induction motor drive insensitive to stator resistance variation. *IEE Proc.-Electr. Power Appl.*, 151(6), 685–693.

Rodriguez, H., Ortega, R., Escobar, G., and Barabanov, N. (2000). A robustly stable output feedback saturated controller for the boost dc-to-dc converter. *Systems & Control Letters*, 40(1), 1 – 8.

Toh, T.T., Mitcheson, P.D., Holmes, A.S., and Yeatman, E.M. (2008). A continuously rotating energy harvester with maximum power point tracking. *J. Micromech. Microeng.*, 18(10), 104008.

Van der Schaft, A.J. (1992). l_2-gain analysis of nonlinear systems and nonlinear state-feedback h∞ control. *IEEE Transactions on Automatic Control*, 37(6), 770–784. URL `http://doc.utwente.nl/29970/`.

Willems, J. (1971). Least squares stationary optimal control and the algebraic riccati equation. *Automatic Control, IEEE Transactions on*, 16(6), 621–634. doi: 10.1109/TAC.1971.1099831.